Combustion, Explosion, and Shock Waves, Vol. 31, No. 5, 1995

FLAME PROPAGATION THROUGH AN ALUMINUM AEROSUSPENSION AT REDUCED PRESSURE

D. A. Yagodnikov, A. V. Voronetskii, and V. I. Lapitskii

UDC 536.46

The rate of flame propagation through an aerosuspension of ASD-1 powdered aluminum is measured in the pressure range 0.1-0.05 MPa and at various component ratios corresponding to a fuel excess. Linear reduction in flame speed with reduction in pressure is observed. It is shown that the combustion of aluminum—air mixture is the most sensitive to pressure change. Spectrozonal cinerecording and optoelectronic image analysis are used to determine the temperature field in the flame front of an overenriched aerosuspension; the formation of eddy structures due to the hydrodynamic interaction of particle settling and the formation and propagation of a combustion surface is recorded.

In the operation of various power stations, the ignition and combustion of gas-disperse systems may occur at an ambient pressure p_0 that differs from atmospheric pressure. Therefore, the influence of pressure on the ignition and combustion of both single metal particles and gas suspensions is investigated experimentally, in order to optimize the parameters of the operating process. Whereas for single particles the delay time of ignition and combustion, the ignition temperature, and several other parameters have been determined at reduced and increased pressure [1-3], experimental investigations of gas suspensions (mainly aerosuspensions) have been conducted at or above atmospheric pressure; see [4-6], for example. Therefore, the aim of the present work is to investigate the ignition and combustion of aerosuspensions of ASD-1 powdered aluminum particles (mean-mass diameter 25 μm) at reduced pressure. The basic quantitative characteristic of the processes here considered is the flame propagation rate W_f through the aerosuspension.

The experiments are conducted on a vertical working section (cross section 80 × 80 mm) with a transparent polymethyl methacrylate front wall. The height of the section is 1500 mm, which permits detailed investigation of the dynamics of flame formation, transformation, and propagation. A window with inset photoresistors for recording ignition of the aerosuspension is placed in the side walls. A VN-461M vacuum pump creates the low pressure in the working section. The pressure and temperature of the flame are measured by means of an MDD200-1000 pressure sensor and a VR5-20 tungsten—rhenium thermocouple, the junctions of which (diameter 0.5 mm) are positioned 10 mm from the wall. Since the diameter of the thermocouple's protective ceramic shell is 2 mm. the influence of the probe on the flame hydrodynamics may be neglected. The converter readings are recorded on an N-117 loop oscillograph.

The method of determining the rate of flame propagation was outlined in detail in [7]. Here it is only necessary to say that the flame propagates upward from the open end to the closed end, and the combustion products are collected in a receiver whose volume is an order of magnitude greater than that of the working section. In this case, there is laminar flame propagation; its rate is calculated by summing the settling rate of the aerosuspension and the rate of flame propagation relative to the walls of the working section. The increase in pressure in the course of the experiment is no more than 15% (~12% in the initial ignition and ~3% in Al combustion). Therefore, the initial pressure value is used in reporting and analyzing the results.

Since, in the experiment, the rate of flame propagation is determined in a settling aerosuspension, the first step is to investigate this process. It is found that the settling rate W_{se} is constant over the length of the working section and increases with decrease in pressure (Fig. 1). Since in the experimental range of Al concentrations (B_{co} = 0.63-2.1 kg/m^3), the mean

N. É. Nauman Moscow State Technical University. Translated from Fizika Goreniya i Vzryva, Vol. 31, No. 5, pp. 23-31, September-October, 1995. Original article submitted June 20, 1994; revision submitted March 1, 1995.

 0010-5082/95/3105-0524$12.50

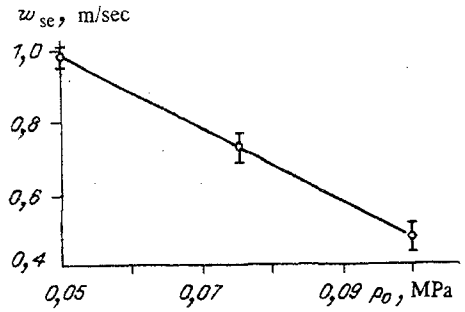

Fig. 1. Pressure dependence of the settling rate.

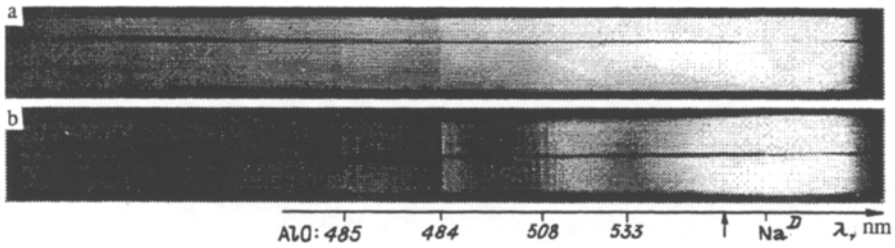

Fig. 2. Spectrograms of the combustion products of an aluminum—air mixture: a) p_0 = 0.075 MPa, α = 0.12; b) p_0 = 0.05 MPa, α = 0.11.

distance between the particles is two orders of magnitude greater than their diameter and, hence, there are few interactions between the individual particles, the result obtained may be explained by the Stokes law

$$F = 6\pi\nu\rho_0 r_s v_s . \tag{1}$$

Here r_s, v_s are the radius and speed of an individual particle; ν, ρ_0 are the kinematic viscosity and density of the air. It follows from Eq. (1) that, other conditions being equal, reduction in ρ_0 leads to reduction in the drag force F acting on the particle. Analysis of a series of experiments shows that the settling rate does not depend on the Al concentration (within the limits of measurement error and with the confidence level of 0.95 adopted in constructing the confidence interval for W_{se} in Fig. 1).

VISUALIZATION AND SPECTRAL ANALYSIS

The use of a transparent front wall permits cinerecording of flame propagation (using a Krasnogorsk-3 camera, 32 frames/sec). The cinerecordings obtained are analyzed optoelectronically [7], permitting conversion of the halftone image into a binary-code equivalent in terms of the degree of darkening of the photoemulsion and its identification with the value of a particular parameter, for example, temperature.

To optimize the cinepyrometric temperature determination, the total radiation spectrum of the combustion products of the aluminum aerosuspension is recorded on an ISP-51 prismatic spectrograph (exposure time ~1.5 sec). In the spectrogram (Fig. 2), an unresolved sodium doublet (589 nm) and AlO oscillatory bands (transition $B^2\Sigma \rightarrow {}^2\Sigma$) with leading quanta of 465, 484, 508, and 533 nm are seen in the visible range against the background of a continuous spectrum from subdisperse aluminum-oxide particles. Accordingly, the temperature characteristics of aerosuspension combustion are obtained by recording the monochromatic brightness of the condensed-phase radiation. To this end, an interference light filter is mounted on the objective of the cine camera. Thus, brightness pyrometry with conversion to the true temperature by means of the Wien formula is employed here [8, 9]. The working wavelength of the cinerecording, corresponding to the transmission maximum of the interference filter (λ_c = 550 nm, as indicated by the arrow in Fig. 2) is chosen in the spectral region where there are no molecular bands, i.e., the radiation may be attributed directly to the condensed phase.

Visualization of flame propagation reveals that, after ignition of the aerosuspension by an electric arc, the flame surface is very extended. However, as the flame moves upward, there is a gradual reduction in its surface area and speed. Beginning at a distance l_{un} = 250-350 mm from the point of ignition, transition to uniform conditions is observed (Fig. 3). This is

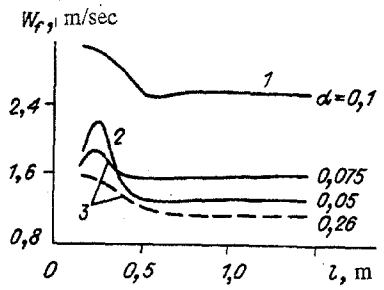

Fig. 3. Variation in combustion rate over the length of the working section: P_0 = 0.1 (1), 0.075 (2), and 0.05 (3) MPa.

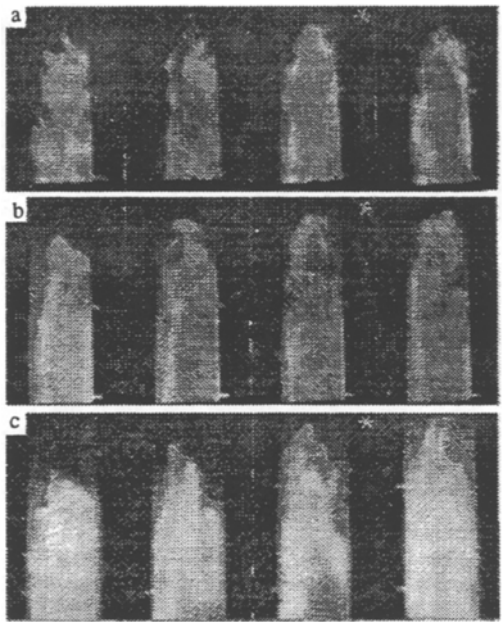

Fig. 4. Cinerecordings of flame propagation: a) p_0 = 0.075 MPa, α = 0.26; b) p_0 = 0.075 MPa, α = 0.13; c) p_0 = 0.05 MPa, α = 0.1; $\Delta\tau$ = 31 msec.

confirmed by calculations of the propagation of a nonsteady flame [10] and agrees with experimental data on the combustion of aerosuspensions of polystyrene, coal, and shale particles [11], according to which the flame accelerates at first and then, after reaching a maximum value W_f, remains practically constant. The presence of transient conditions may be explained by the influence of the ignition system on the initial stage of flame formation: the considerable power (~1.5 kW) liberated by the ignition system intensifies the heating and ignition of the Al particles. Theoretical estimates on the basis of a radiational model of a flame [10, 11] show that the characteristic scale at which steady laminar-flame motion sets in may be assumed to be the radiation path length of the combustion products

$$l_{un} = 1{,}5\, r_s \rho_s / B_{co}, \quad B_{co} = \rho_0/(K_m \alpha), \tag{2}$$

where ρ_3 is the particle density; K_m is the mass stoichiometric ratio; the coefficient α characterizes the oxidant excess in the working section.

On the other hand, monotonic increase in speed is prevented by the near-laminar settling conditions of the aerosuspension. Thus, in the experimental conditions, the Reynolds number, calculated from the settling rate and the equivalent tube diameter, is 2600 (p_0 = 0.1 MPa) and 2900 (p_0 = 0.05 MPa). In addition, if high-speed flame propagation is to occur, the turbulence generated by the walls must reach the flow core, which may occur at distances of ~25 tube diameters (~2.2 m

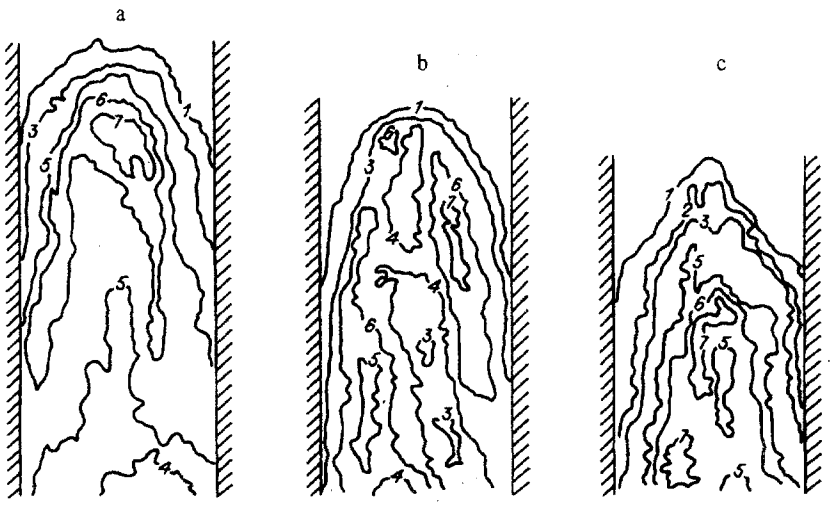

Fig. 5. Isotherms in the working section: 1) 1930 K; 2) 2120 K; 3) 2290 K; 4) 2440 K; 5) 2580 K; 6) 2650 K; 7) 2720 K.

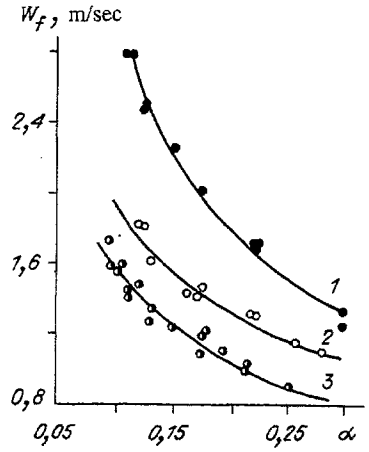

Fig. 6. Dependence of the combustion rate on the component ratio: p_0 = 0.1 (1), 0.075 (2), and 0.05 (3) MPa.

in the present case) [12]. Therefore, the length of the working section is not sufficient for closure of the turbulent boundary layers.

Cinerecordings of flame propagation in steady conditions are shown in Fig. 4. It is evident that the surface has a complex dome shape and changes only slightly as the flame moves. The source of the perturbations observed is most likely that settling of aerosuspension with a sufficiently large content of disperse phase is accompanied by the opposing motion of gas microvolumes and the formation of eddy structures. As a result, the front boundary of the settling aerosuspension has a local turbulizing action on the flame. The hydrodynamic features of flame propagation recorded here are in satisfactory agreement with the data of [13], in which concurrent motion of the air, the appearance of a convective cell, and autoturbulization of the aerosuspension were established by visualization of the settling process using dust. As a result, it is difficult, if not impossible, to determine the normal flame speed, which is one of the fundamental characteristics of combustion, with satisfactory accuracy in the overenriched aerosuspension.

The results of optoelectronic analysis of the cinerecordings marked by an asterisk in Fig. 4 are shown in Fig. 5 in the form of isotherms. For the analysis, the surface of the flame front may be assumed to be the region of the flame bounded by the leading 1930 K isotherm, which corresponds to the photometric sensitivity of spectral cinerecording and the maximum temperature gradient. The characteristic feature of the flame structure is the presence of a temperature range 150-200 K above the equilibrium value (α = 0.26, p_0 = 0.075 MPa, T* = 2500 K). In the wake of the flame front, the temperature falls to

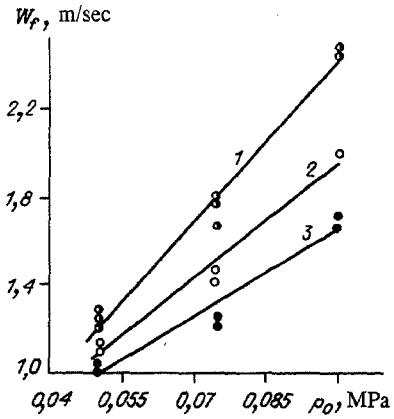

Fig. 7. Pressure dependence of the combustion rate: α = 0.11-0.13 (1), 0.16-0.18 (2), and 0.22-0.24 (3).

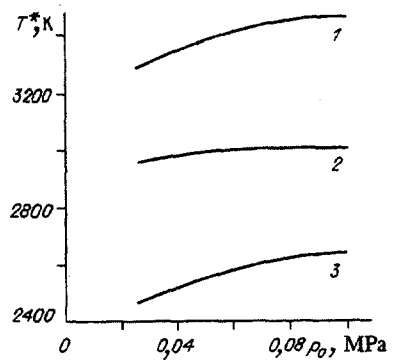

Fig. 8. Pressure dependence of the adiabatic combustion temperature: α = 0.7 (1), 0.5 (2), and 0.1 (3).

~2400 K. This is obviously because polydisperse Al is used and the smallest Al particles ignite before the others and burn with a local component ratio characterized by larger α. Eddy formation also leads to the appearance of zones with a component ratio that differs from the mean. In addition, the radiation of the subdisperse aluminum-oxide particles is determined by the temperature at which they are formed, which is ~3900 K (chemical condensation of Al_2O_3), according to [14].

Measurements of the flame are also made by two thermocouples that are 500 mm apart. Since the characteristic time of flame propagation is ~1 sec, temperature measurement by the thermocouples is associated with considerable error, because of their inertia. For example, a maximum temperature of ~1220 K (α = 0.26, p_0 = 0.075 MPa) is recorded ~3 sec after the flame passes the site of the lower thermocouple. The readings of the thermocouple that is closer to the upper end of the working section is ~300 K lower, since its contact time with the combustion products is less. The significant difference in the results of radiant and probe pyrometry is explained in that, in the combustion of powered Al, material settles on the junctions, and the thermocouples are close to the wall of the apparatus, where they feel the influence of the boundary layer. Thus, the temperature values recorded by thermocouple probing of fast ignition and combustion of aerodisperse systems are too low.

INFLUENCE OF COMPONENT RATIO

With increase in Al concentration (reduction in oxidant excess coefficient), the rate of flame propagation increases (Fig. 6). This is due to increase in the volume concentration of particles and the bulk heat liberation, which leads to increase in the conductive and radiant heat fluxes heating the initial aerosuspension. In addition, the temperature of aerosuspension ignition falls with decrease in α [15], and exothermal nitriding occurs in the overenriched aerosuspension with burnup of oxygen. As

TABLE 1. Relative Mass Content of Active Aluminum in Combustion Products

p_0, MPa	α				
	0,1	0,13	0,17	0,21	0,28
0,05	0,63	0,64	0,61	0,71	—
0,075	—	0,48	0,53	0,47	0,48
0,1	—	0,35	0,29	0,33	0,31

a result, the combustion temperature of the aerosuspension increases, condensed aluminum nitride appears in the combustion products, and the upper concentrational range of flame propagation expands [16].

Visualization by cinerecording reveals an additional factor responsible for the increase in W_f. As is evident from Fig. 4b, the distortion of the flame front increases with decrease in α, which leads to increase in the surface and hence in the combustion rate. However, it is hard to determine which factor predominates, on account of the close relation between the individual stages of the process and the experimental conditions in the case of an overenriched aerosuspension.

Study of the transition to uniform flame propagation shows that the extent of the nonsteady section remains constant with decrease in α (Fig. 3). This result contradicts Eq. (2), at first glance, but most likely confirms a complex mechanism of flame-front formation, with the participation of radiant, conductive, and hydrodynamic factors.

Optoelectronic analysis of the cinerecordings shows that the internal flame structure is also complicated, as indicated by the formation of low-temperature zones in the flow core (Fig. 5b). Nevertheless, the region of maximum temperature is close to the tip of the flame front, as before.

Note also that the displacement of the $W_f(\alpha)$ curve toward the overenriched aerosuspension agrees with experimental data for aerosuspensions of different disperse and chemical compositions [4, 5, 12, 13, 17].

INFLUENCE OF PRESSURE

With reduction in pressure in the working section, the basic laws of flame propagation remain unchanged. The flame is still dome-shaped and perturbations with practically the same characteristic dimension are again seen at the surface (Fig. 4c). An analogous result was obtained in [18] in investigating the influence of pressure on the turbulence parameters and the turbulent combustion of hydrocarbon fuel: the scale of the turbulence does not depend on the pressure (in the range p_0 = 0.06-0.01 MPa). Note also that, in this case, the presence of disperse-phase particles leads to quenching of the pulsations that appear.

Nevertheless, some differences are noted: in particular, the rate of flame propagation in steady conditions is lower. As is evident from Fig. 7, $W_f(p_0)$ may be satisfactorily approximated (with a dispersion no greater than 5.6%) by linear functions in the range α = 0.11-0.23

$$W_f = -0{,}02 + 24{,}5p_0, \quad \alpha = 0{,}11 - 0{,}12,$$
$$W_f = 0{,}22 + 17{,}3p_0, \quad \alpha = 0{,}16 - 0{,}18,$$
$$W_f = 0{,}34 + 13{,}1p_0, \quad \alpha = 0{,}22 - 0{,}23.$$

The $W_f(p_0)$ curves may be explained by the influence of pressure on the ignition and combustion of Al particles. It was established in [19] that, in the heating of aluminum in oxygen, reducing the oxygen pressure is associated with reduction (by 5-10%) in the rate of low-temperature oxidation. In addition, in accordance with calculations of the characteristics of the speed and temperature disequilibrium of the aerodisperse flame front by the two-continuum model [5], reduction in pressure from 0.1 to 0.05 MPa leads to decrease in Nusselt number from 2.63 to 2.32 (for particles of diameter 20 μm) and hence in the heat-transfer coefficient on heating the particles. Therefore, it may be assumed that the delay period increases somewhat with decrease in pressure. Note that the inhibiting influence of pressure may partially compensate the reduction in temperature of the Al particle at the instant of ignition, with a corresponding reduction in the Al vapor pressure (most significantly when $p_0 \leq 0.05$ MPa), as indicated by the data of [20, 21].

On the other hand, with reduction in pressure in the given range, the adiabatic combustion temperature of the aerosuspension falls by 150-200 K (Fig. 8). This is confirmed by reduction in intensity of the continuous radiation spectrum of the condensed phase, against the background of which the AlO molecular bands are more clearly distinguished (Fig. 1b).

Chemical analysis of the combustion products of the aerosuspension indicates an increase in content of active aluminum in the condensed phase (Table 1), which implies less complete combustion of the Al. In addition, according to the three-zone model of Al-particle combustion [22], the mass rate of combustion decreases in proportion to the decrease in pressure, since the diffusional permeability (with respect to oxidant molecules) of the zone of chemical condensation of Al_2O_3 surrounding the particle decreases in this case. As a result, the heat-flux gradients at the flame front and the intensity of heat transfer between the combustion products and fresh aerosuspension decrease. This is confirmed by the temperature distribution (Fig. 4c), from which it follows that the zone with the greatest temperature is shifted from the tip of the front to the depth of the flame (the 2720 K isotherm).

Another feature of flame propagation at reduced pressure is an increase in the maximum apparent flame speed and hence in W_f in the nonsteady section, although the extent of this section is hardly changed (Fig. 3). For example, when α = 0.13-0.14 and p_0 = 0.1, 0.075, 0.05 MPa, W_f^{max}/W_f = 1.13, 1.18, 1.65, respectively. The increase in W_f^{max} is probably due to reduction in the damping influence of the atmosphere (reduction in viscosity of the air with decrease in the pressure) and slowing of speed and thermal relaxation.

To sum up, the influence of reducing the pressure in the working section on individual macrokinetic stages of flame propagation leads to decrease in W_f. The combustion of Al is most sensitive to change in the pressure. Visualization permits study of the flame structure and flame propagation in an overenriched aerosuspension; it is found that there is a hydrodynamic relation between the settling of the particles and the formation of the combustion surface.

REFERENCES

1. I. M. Kar'yanov, V. I. Malinin, and E. I. Kotel'nikova, "Influence of the pressure on the ignition of boron with various constants of oxidation," Fiz. Goreniya Vzryva, **18**, No. 5, 98-101 (1982).
2. E. A. Valov, E. I. Gusachenko, and V. I. Shevtsov, "Influence of the pressure on the ignition of individual magnesium particles in carbon dioxide," in: Chemical Physics of Combustion and Explosion. Combustion of Heterogeneous and Condensed Systems [in Russian], Chernogolovka (1989), pp. 85-87.
3. A. V. Florko, V. V. Golovko, and A. N. Pisarenko, "Combustion of single particles," Fiz. Goreniya Vzryva, **22**, No. 2, 25-40 (1986).
4. V. M. Kudryavtsev, A. V. Sukhov, A. I. Vyatkin, et al., "Propagation of the chemical reaction front in a two-phase flux," in: Production and Diagnostics of High-Temperature Gas Fluxes [in Russian], Khar'kovsk. Aviats. Institut im. N. E. Zhukovskogo (1987), No. 4, pp. 66-69.
5. D. A. Yagodnikov and A. V. Voronetskii, "Influence of nonequilibrium speeds on the propagation of a laminar flame in an aerodisperse medium," Fiz. Goreniya Vzryva, **28**, No. 5, 38-44 (1992).
6. N. N. Yanenko, V. M. Fomin, A. V. Fedorov, et al., "Structure of shock and detonation waves and combined discontinuities in gas—particle mixtures," in: Mechanics of Reacting Media and Its Application [in Russian], Nauka, Novosibirsk (1989), pp. 133-143.
7. D. A. Yagodnikov, A. V. Voronetskii, V. M. Mal'tsev, and V. A. Seleznev, "Increasing the propagation rate of the flame front in an aluminum aerosuspension," Fiz. Goreniya Vzryva, **28**, No. 2, 51-54 (1992).
8. A. N. Bobrov, D. A. Yagodnikov, and I. V. Popov, "Ignition and combustion of two-component gas-suspension of powered fuel and oxidant," Fiz. Goreniya Vzryva, **28**, No. 5, 3-7 (1992).
9. V. M. Mal'tsev, M. I. Mal'tsev, and L. Ya. Kashporov, Basic Characteristics of Combustion [in Russian], Khimiya, Moscow (1977).
10. L. I. Ivanishcheva and A. M. Stepanov, "Nonsteady flame propagation through a gas suspension of solid-fuel particles," Fiz. Goreniya Vzryva, **13**, No. 5, 699-705 (1977).
11. O. M. Todes, A. D. Gol'tsiker, and K. K. Ionushas, "Formation and development of a flame front in aerodisperse systems," Fiz. Goreniya Vzryva, **10**, No. 1, 83-88 (1974).
12. M. A. Andreev and A. M. Stepanov, "Modeling the propagation of a nonsteady turbulent flame through an aerosuspension of metallic particles," Fiz. Goreniya Vzryva, **22**, No. 6, 37-46 (1986).
13. S. V. Goroshin, V. G. Shevchuk, L. V. Boichuk, et al., "Laminar flame of aerosuspensions in tubes," in: Macroscopic Kinetics, Chemical and Magnetic Gas Dynamics [in Russian], TGU, Tomsk (1991), part 12, pp. 140-141.
14. W. G. Parcker and H. G. Wolfhard, "Emissivity of small particles in flame," Nature, **162**, No. 4111, 259 (1948).

15. S. N. Afanas'ev, V. Yu. Zhar'kov, and E. S. Ozerov, "Ignition and combustion of a gas suspension of aluminum particles," in: Physics of Aerodisperse Systems [in Russian], Kiev (1985), no. 27, pp. 39-42.
16. D. A. Yagodnikov, A. V. Sukhov, V. I. Malinin, and I. M. Kir'yanov, "Role of nitriding in flame propagation through an over-enriched metal—air mixture," Vestn. MGTU, Ser. Mashinostr., No. 1, 121-124 (1990).
17. L. D. Smoot and H. D. Horton, "Flame propagation in the coal dust," Prog. Energy Comb. Sci., **3**, No. 4, 235-239 (1977).
18. V. A. Khrampov, "Influence of pressure on the turbulence parameters and on turbulent combustion," in: Combustion at Reduced Pressure and Flame Stabilization in Homogeneous and Two-Phase Systems [in Russian], Izd. AN SSSR, Moscow (1960), pp. 43-57.
19. E. A. Gulbransen and W. S. Wysong, "Thin oxide films on aluminum," J. Phys. Chem., **51**, No. 9, 1087-1103 (1947).
20. D. K. Kuel, "Ignition and combustion of aluminum and beryllium," AIAA J., **3**, No. 12, 2239-2247 (1965).
21. T. A. Brzhustovskii and I. Glassmen, "Vapor-phase diffusional flames in the combustion of magnesium and aluminum," in: A. V. Il'inskii (Editor), Heterogeneous Combustion [Russian translation], Mir, Moscow (1967), pp. 126-164.
22. V. M. Kudryavtsev, A. V. Sukhov, A. V. Voronetskii, and A. P. Shpara, "Combustion of metals at high pressure (three-phase model)," Fiz. Goreniya Vzryva, **15**, No. 6, 50-57 (1979).